JOURNAL OF COASTAL AND HYDRAULIC STRUCTURES

Vol. 6 , 2026, 53

Internal Erosion in a Full-Scale Experimental Embankment Dam: Insights from the Dismantling of the Älvkarleby Test Dam

Lagerlund, J. [1*], Viklander, P.[2] and Toromanović, J. [3]

[1] Vattenfall R&D, Sweden
[2] Hydroresearch AB, Sweden
[3] Mining and Geotechnical Engineering, Department of Civil, Environmental and Natural Resources Engineering, Luleå University of Technology, Sweden
[*] johan.lagerlund@vattenfall.com

Research Article. **Submitted:** 17 February 2026. **Reviewed:** 23 April 2026, 1 June 2026. **Accepted** after double-anonymous review: 5 June 2026. **Published:** 17 July 2026.

DOI: 10.59490/jchs.2026.0053

Cite as:. "Lagerlund, J., Viklander, P., & Toromanovic, J. Internal Erosion in a Full-Scale Experimental Embankment Dam: Insights from the Dismantling of the Älvkarleby Test Dam. Journal of Coastal and Hydraulic Structures. https://doi.org/10.59490/jchs.2026.0053"

32nd EWG-IE Meeting
7th EWG-OOE Meeting
Delft, the Netherlands
22-26 June 2026

This paper is part of the **Thematic Series** of work presented at the joint meeting of the European Working Groups on Erosion. Guest editor was André Koelewijn.

ISSN: 2667-047X online

Abstract

Internal erosion is a leading cause of embankment dam failure, yet its mechanisms remain difficult to observe directly. This study presents findings from the dismantling of a 4.1 m high, full-scale experimental embankment dam constructed in Älvkarleby, Sweden, with embedded defects. The dam featured a moraine core, protected by fine and coarse filters and supported by rockfill. After 4.5 years of operation, the dam was dismantled, revealing multiple internal erosion features despite adherence to modern design standards.

Key observations include a sinkhole-like feature with a softened, saturated zone underneath it, coinciding with one of four horizontally installed strain cables. Three horizontal erosion pipes were identified underneath a vertical coarse-column defect, aligned along horizontal core layer boundaries. A sandy zone near a wooden block defect and thin, sand-filled streaks at core layer boundaries were also documented, suggesting early-stage erosion along construction-induced stratification planes. Along the right abutment, a contiguous zone of disturbed core material and multiple small sinkholes were observed adjacent to the concrete wall.

Sieve analyses revealed both enrichment and depletion of fines in the downstream fine filter, highlighting variability in retention performance. Coarse filter segregation and core–fine filter incompatibility was suspected to contribute to a two-stage erosion mechanism. These findings underscore the critical role of construction-induced heterogeneities, moisture variability, and filter placement in internal erosion development. The study emphasizes the need for improved construction control, real-time monitoring, and post-construction verification to improve long-term embankment dam performance.

Keywords

Internal erosion, Embankment dams, Full-scale testing, Filter performance, Construction-induced heterogeneity.

1 Introduction

Internal erosion is one of the primary causes of embankment dam failures worldwide. It is a progressive process that can lead to leakage, sinkholes, and structural instability if not detected and mitigated in time (ICOLD, 2017; Foster *et al.*, 2000). In Sweden, most large hydropower dams were constructed between the 1940s and 1970s as zoned embankments with central moraine cores and filter layers (Cederström, 1995; RIDAS, 2012). Although these dams were built to the standards of their time, aging infrastructure and evolving operational demands have heightened the urgency of addressing internal erosion risks (Lagerlund, 2024). Early detection of performance changes has therefore become a key priority in dam safety management (Johansson and Nilsson, 2005; RIDAS, 2020).

Traditional monitoring methods, such as visual inspection, piezometric readings, and seepage measurements, often fail to detect internal erosion before visible signs appear (Viklander *et al.*, 2023). This has driven the development of non-destructive testing and advanced monitoring techniques for embankment dams (Toromanović *et al.*, 2022a; Johansson, 1997). The Älvkarleby test embankment dam was constructed in 2019 as part of Vattenfall AB's Hydro R&D Programme "Dam Safety and Infrastructure" to evaluate whether such methods can detect anomalies in dams under controlled conditions. The project involved Vattenfall, Luleå University of Technology, Uppsala University, Lund University of Technology, and HydroResearch AB, and was co-funded by Energiforsk's Dam Safety Programme and the Swedish Hydropower Centre (SVC).

The dam was built inside a 20 m × 16 m × 4 m concrete containment box (see Figure 1) and designed as a zoned embankment dam with a central moraine core, fine and coarse filters, and rockfill shoulders. The side walls of the concrete containment box were inclined outward at a slope of 8V:1H to improve compaction at the core–abutment interface. This is the common practice when constructing new abutments in embankment dams (RIDAS, 2012). Bentonite-enriched mastic was applied at the abutments to reduce preferential seepage paths and emulate the contact grouting used in full-scale dams (Fell and Fry, 2007; Lowe, 1997).

Five intentional defects were embedded in the core soil to simulate internal weaknesses: two horizontal gravel layers, a vertical coarse column, a buried concrete block, and a wooden cube inclusion (Lagerlund *et al.*, 2022). Multiple research teams applied non-invasive monitoring techniques, including electrical resistivity tomography, distributed fibre-optic sensing (temperature and strain), seismic surveys, and ground-penetrating radar, to detect the embedded defects (Viklander *et al.*, 2023; Norooz *et al.*, 2024). These efforts were supported by pre-construction modelling of the dam's electrical, thermal, and seismic responses (Dahlin *et al.*, 2019; Johansson and Sjödahl, 2018).

Figure 1. Construction of the test dam inside the concrete containment box in 2019.

The reservoir was impounded in early 2020 and maintained at a near-constant level of ~3.27 m above the base (20 cm below the core crest) for two years, marked with a blue line labelled "Water level" in Figure 2. In 2022, five short controlled drawdown-refill cycles were conducted to simulate operational fluctuations (Toromanović *et al.*, 2025), followed by remedial grouting trials using a novel non-hardening grout material (Lagerlund, 2024; Lagerlund *et al.*, 2023). The dam was dismantled in autumn 2024 in 0.4 m vertical increments, with detailed documentation of observed features (Lagerlund and Riaz, 2026).

This paper aims to investigate the mechanisms and contributing factors underlying the internal erosion features observed during dismantling. By linking these findings to construction records, material properties, and monitoring data, the study aims to explain how design choices, construction practices, and environmental conditions influenced the development of internal erosion. The results contribute to the fundamental understanding of internal erosion in dams and inform recommendations for future experimental dam design and construction.

2 Construction history of the test dam

Investigations of internal erosion in embankment dams consistently highlight the importance of understanding the dam's design and construction history when diagnosing root causes (Fell and Fry, 2007; FERC, 2021). Many failures or incidents linked to internal erosion can be traced to construction-related vulnerabilities, such as poorly compacted zones, inadequate material transitions, or embedded flaws (Foster *et al.*, 2000; Fry, 2018). Forensic studies therefore emphasise reviewing construction documentation, including design drawings, daily logs, material test results, and as-built records, to identify deviations or weak points that may have served as initiation sites for seepage and internal erosion (FERC, 2021).

In the Älvkarleby test embankment dam, construction was thoroughly documented in a daily log, offering detailed insight into how the dam was built and quality-controlled. This record enables the identification of potential factors that contributed to the internal erosion features observed four years later during dismantling. Key aspects include material characteristics (gradation, compaction, moisture content), construction procedures (layer thickness, applied compaction energy), environmental conditions (temperature, precipitation), and any anomalies or deviations noted. Internal erosion typically initiates where hydraulic gradients intersect erodible materials in the absence of adequate filter protection (ICOLD, 2017; Fell and Fry, 2007). Thus, any construction shortcoming that created a low-density zone, gap, or segregation of fines could later evolve into an erosion conduit under operational hydraulic conditions.

2.1 Dam design and zoning

The Älvkarleby test embankment dam was constructed in 2019 as a zoned rockfill embankment in accordance with Swedish dam safety guidelines (RIDAS, 2012). The dam measured approximately 4.1 m in height and 20 m in length, with a 15 m base width, 3 m crest width, and 1V:1.5H slopes (see Figure 2). The reservoir level was kept at steady-state level of 3.27 m, 0.2 m below the core crest over 4.5 years. Accordingly, the global hydraulic gradient through the core was mild, rising gradually from 0 at the phreatic line to 0.15 (1 m depth), 0.9 (2 m depth), 1.5 (3 m depth), 1.8 (3.6 m depth) and 2 (4.1 m depth).

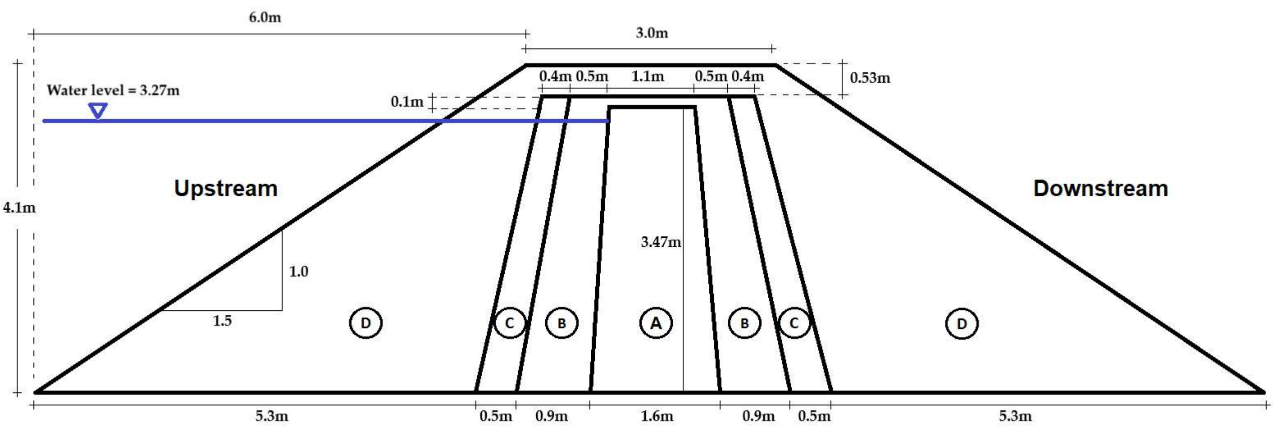

Figure 2. Cross section of the test dam, zone (A) = moraine core soil, zone (B) = fine filter, zone (C) = coarse filter and zone (D) = rockfill.

The central core was designed with a moraine (0–20 mm), with approximately 20% fines (<0.063 mm), sourced from a nearby borrow area and characterized through laboratory testing. Modified Proctor tests indicated an optimum water content of approximately 6% and a maximum dry density of 2200 kg/m³ (Bernstone *et al.*, 2021). The core was flanked by a fine filter (0–16 mm crushed rock material) and a coarse filter (8–64 mm crushed rock material), both designed to meet RIDAS (2012) filter criteria and retain eroded particles (Viklander *et al.*, 2023). Outside the filters, rockfill shoulders (32–150 mm) provided structural support. This zoning closely reflects full-scale Swedish dams, with filter gradations and thicknesses selected to prevent particle migration (Toromanović *et al.*, 2020). Particle size distributions for all dam materials from the design phase are shown in Figure 3.

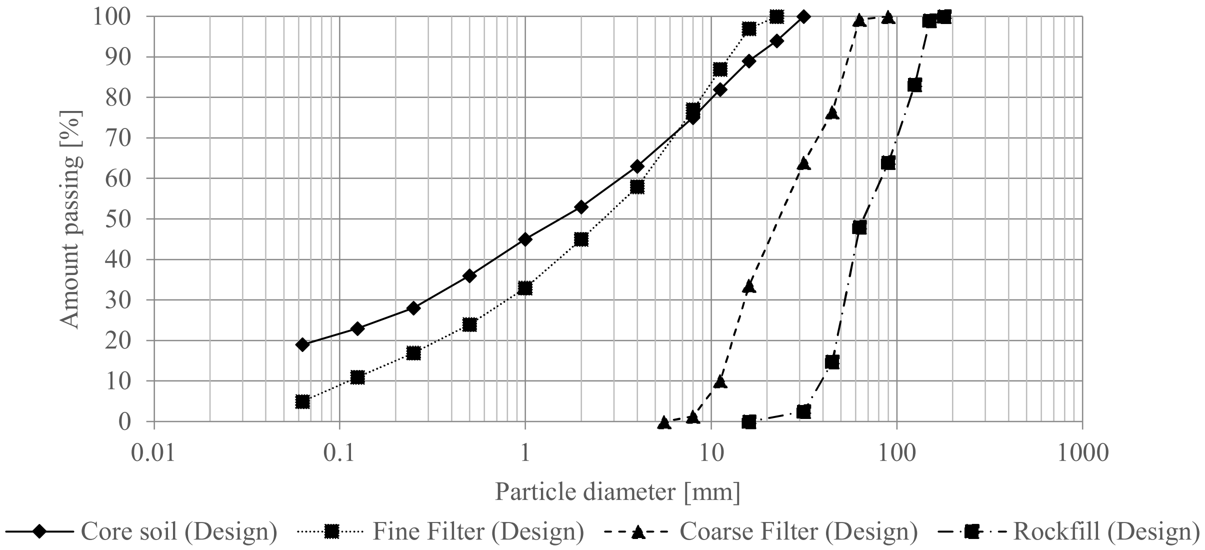

Figure 3. Design curves for the involved dam materials.

2.2 Construction procedure and quality control

Construction of the dam was completed over four weeks in October–November 2019 and followed a systematic, layer-by-layer approach to replicate full-scale dam construction practices. The dam was built in horizontal layers, moving upward in a repeated sequence: core soil first, followed by fine filter, coarse filter, and finally rockfill. Each layer cycle started with placing and compacting the moraine core soil, then adding the fine filter, coarse filter, and rockfill shoulder. This sequence was repeated until the full dam height was reached. The moraine core was placed in layers about 0.3 m thick and compacted to about 0.2 m using a 90 kg vibratory plate compactor. Typically, 4–6 passes were applied per layer, with additional effort near the inclined concrete sidewalls to ensure adequate compaction. Before placing each new core soil layer, the surface of the previous one was roughened to improve bonding and reduce the risk of weak horizontal joints.

For each core layer, two measurement points along its central line were established to assess compaction quality. At each point, compaction and dry density were measured using the water volumetric method, following SS 027110. Water content was measured according to SS-EN ISO 17892-1:2014/A1:2022. About 10 kg of material was collected at each point and stored in buckets for later lab analysis of particle size distribution, performed in accordance with SS-EN ISO 17892-4:2016. Dry density of the core soil ranged from 1940 to 2080 kg/m^3 (88 to 95% of maximum) and fine content from 25% to 30% of weight. The fine and coarse filters were placed in ~0.25 m layers and compacted to ~0.2 m using the same equipment. For each filter layer, particle size distribution was estimated at two locations on both the upstream and downstream side. The rockfill shoulders were placed in 0.3 m layers without compaction, in accordance with standard practice for coarse rockfill shoulders (RIDAS, 2012).

This high-resolution construction and testing protocol provided a detailed dataset on the as-built condition of the dam, including material gradation, compaction quality, and spatial variability. These records were essential for interpreting the internal erosion features observed during dismantling and for evaluating the performance of the dam's filter system and core integrity.

2.3 Embedded defects and environmental conditions

Five artificial defects were embedded during construction:

1. A 0.1 x 0.1 m horizontal layer of permeable 4–8 mm gravel through the core soil at the left abutment.
2. A 0.5 m concrete cube.
3. A vertical column (0.3 m diameter) of loosely compacted 8–64 mm gravel from 1 m height to the core soil crest.
4. A 0.5 x 0.2 m horizontal layer of permeable 4–8 mm gravel through the core soil.
5. A 0.4 m wooden cube.

All locations of the defects are shown in Figure 4. Only the two horizontal gravel layers were surrounded by compacted fine filter to ensure long-term stability, while the other three defects were embedded without any protective fine filter. These embedded defects created intentional material gaps and density differences to simulate internal weaknesses and test how well the monitoring methods and filters worked.

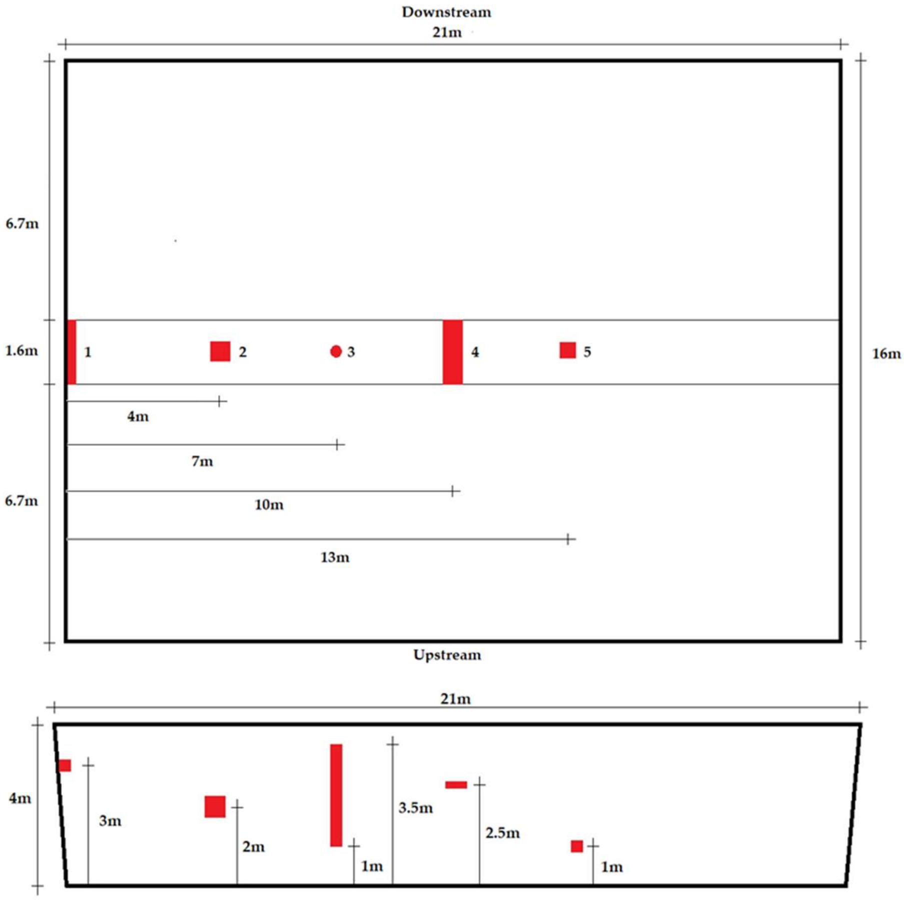

Figure 4. Placement of the defects viewed from above (top) and from upstream to downstream (bottom), (Lagerlund and Riaz, 2026).

Construction was affected by difficult weather, which is common in Swedish autumn. The first two weeks were rainy (~5 °C), followed by sub-zero temperatures. To stop freezing, the exposed core crest was covered each night with Styrofoam and tarpaulin. Even with these precautions, small amounts of snow and ice got into the coarse filter and rockfill during the last two weeks of construction, especially during an early winter storm (Toromanović *et al.*, 2022b). After the finalized construction of the dam, an uninsulated tent was erected above it to protect it from precipitation. The goal was to make sure that seepage measurements downstream of the dam only captured actual seepage, not rainwater.

3 Dismantling methodology

The Älvkarleby test dam was dismantled between 16 September and 3 October 2024, following 4.5 years of operation. Excavation was done in 0.4 m layers, starting with the rockfill and filter zones and ending with the core. The reservoir was drained from full level and left untouched for three weeks before dismantling began. Excavation was carried out using an 18-ton tracked excavator. At first, the machine stood on the crest with its tracks on both sides of the exposed core. After the first metre of crest material was removed, the excavator was relocated to the downstream shoulder.

A sampling and documentation plan was used to collect all important signs of internal erosion:

- Both machine and hand digging were used, with hand tools in areas likely to have erosion or unusual features.
- A trained expert watched the whole excavation process closely.
- Undisturbed core samples were taken both vertically and horizontally at different depths.
- Sieve analysis of core and fine filter materials to assess particle size distribution.
- In situ dry density and water content measurements at depths of 1.0 to 3.8 m on both upstream and downstream sides of the core.
- Sampling of the downstream fine filter at depths of 1.0 to 3.8 m and at three locations: left abutment, centre, and right abutment.
- Sieve analysis of eroded material from filled sinkholes, pipes, sandy zones, and washed-out fine filters.
- Photo documentation and mapping of all anomalies, including depth, orientation, and extent.
- The height of the crest and the 12 piezometers (installed at five levels in the core) were measured.

This systematic approach ensured that relevant signs of internal erosion were captured and preserved for subsequent analysis. The results from the core sample tests are not included in this paper.

4 Observed internal erosion

4.1 Settlements of the core crest and pore pressure transducers

Settlements in the dam body were observed during dismantling. The core crest had differential settlements up to 10 cm, see Figure 5. At time of construction in 2019, the height of the core soil was at 347 cm with a tolerance of ± 5 mm. No settlements were seen before dismantling, except at one inclinometer in the downstream rockfill slope. Several laser scanning campaigns were done 2019 – 2024. The laser scans had a resolution of about 1 mm.

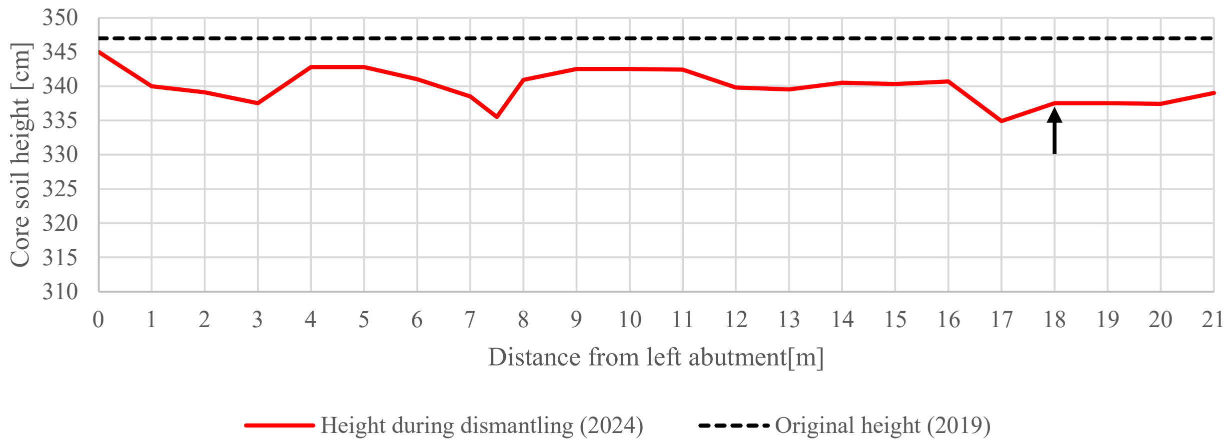

Figure 5. Core soil height at time of dismantling, (Lagerlund and Riaz 2026). Piezometer section marked with black arrow.

The piezometers were installed in one single section of the dam, 3 m in from the right abutment. Their installation depths and locations within this section is shown in Figure 6. Eleven of the twelve piezometers installed in the core and filter zones were recovered and found to have settled from their original installation depths. Settlements ranged from approximately 5 to 10 cm, with the biggest relative movements in the lower core and the largest total settlements at the top, see Table 1.

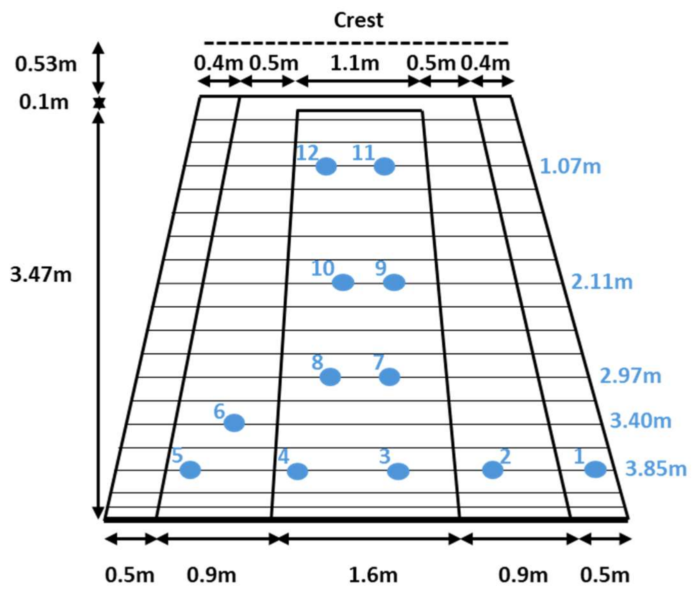

Figure 6. Location and approximate depth of the 12 piezometers installed in one section of the dam, 3.0 m in from the right abutment. Upstream to the left and downstream to the right.

Table 1. Level measurements of the piezometers at time of installation 2019 and dismantling 2024, (Lagerlund and Riaz, 2026)

Location	Piezometer	Depth 2019 [m]	Depth2024 [m]	Difference [cm]	Relative settlement[1] [%]
DS coarse	1	3.850	3.875	-2.5	9.5
DS fine	2	3.863	3.894	-3.1	12.4
DS core	3	3.863	3.886	-2.3	9.4
US core	4	3.864	3.903	-3.9	15.9
US fine	5	3.836	3.868	-3.2	11.8
US fine	6	3.404	lost		
DS core	7	2.971	3.043	-7.2	6.4
US core	8	2.975	3.052	-7.7	6.8
DS core	9	2.105	2.211	-10.6	5.3

US core	10	2.125	2.236	-11.1	5.6
DS core	11	1.069	1.165	-9.6	3.2
US core	12	1.074	1.179	-10.5	3.5

[1]Calculated as measured settlement divided by height from the base.

While pore pressures were monitored continuously throughout the dam's operation (Toromanović, 2024), their time-series analysis falls outside the scope of this forensic study; here the transducers serve only as internal reference points for vertical settlement between installation and dismantling

4.2 Erosion features and material redistribution

Multiple internal erosion features were documented throughout the dam body during dismantling:

A *developing sinkhole-like feature* (about 300 litres in volume) was found between levels 1.4–0.2 m above the base, approximately 17.5 m from the left abutment, see Figure 7. The feature was filled with eroded core material, with finer particles concentrated in the upper portion and coarser material at the bottom, see Figure 8. Beneath the sinkhole, at approximately 0.2 m above the base, a very wet and softened zone was encountered, approximately 1 m wide. This area was located between two of the four pre-stressed strain cables installed horizontally through the core at 0.15 m height with a one meter spacing.

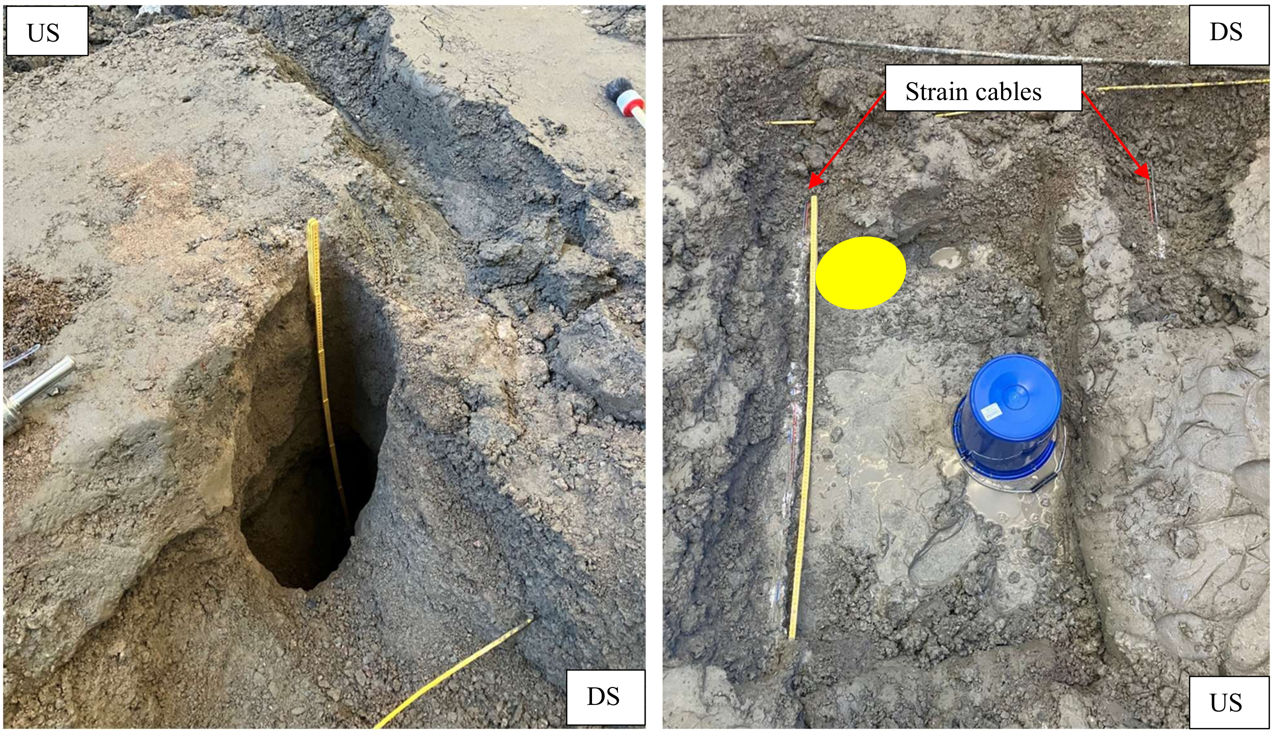

Figure 7. To the left: sinkhole-like feature with its eroded core soil material removed. To the right: Wet, damaged core soil beneath the sinkhole-like feature. Bottom of the sinkhole-like feature marked with a yellow circle, (Lagerlund and Riaz, 2026).

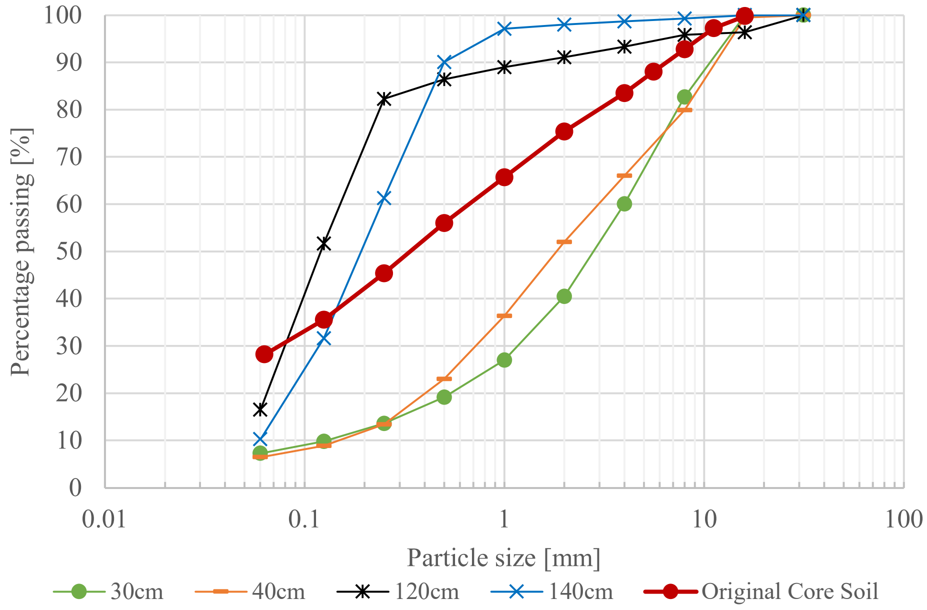

Figure 8. Particle size distribution curves show that eroded core soil sampled from higher parts in the sinkhole-like feature (140 and 120 cm above the base of the containment box) was more fine graded than eroded core soil near the bottom (40 to 30 cm). Fine material had been washed out in all locations compared with the original particle size distribution of the core soil (mean value from all tested core soil layers during construction), (Lagerlund and Riaz, 2026).

Three horizontal erosion pipes were observed underneath the base of the vertical coarse column defect. These were located along horizontal layer boundaries and contained coarse sand and fine gravel, see Figure 9. In addition, signs of erosion were also observed at the top of the vertical defect, near the crest of the core soil.

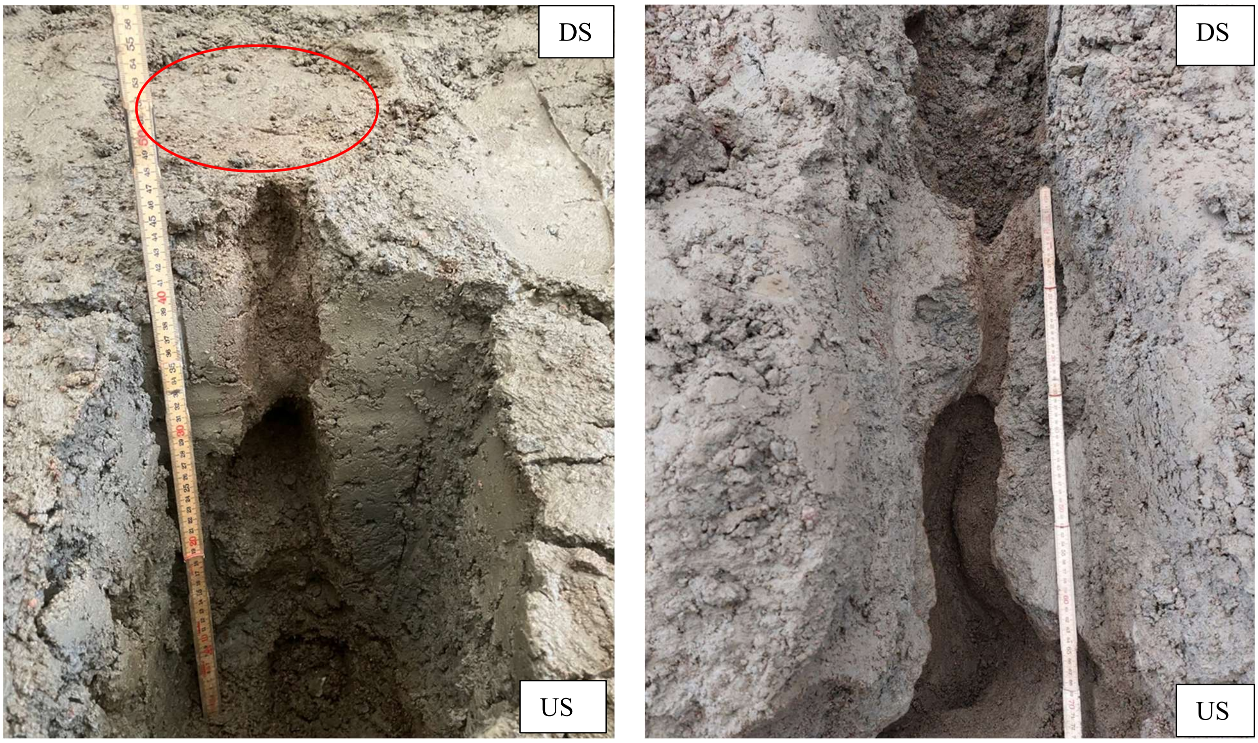

Figure 9. To the left: Erosion at three different levels under the vertical defect (red circle). To the right: The core soil "roof" of the middle pipe removed. After the eroded soil was removed, the damage had the shape of an hourglass with the waist located ca 20 cm below the bottom of the vertical defect, (Lagerlund and Riaz, 2026).

A sandy zone (~1 m long, ~40 cm high) was found near the wooden block defect at level ~1 m, starting at the core–downstream fine filter interface but did not traverse the core soil completely, see Figure 10.

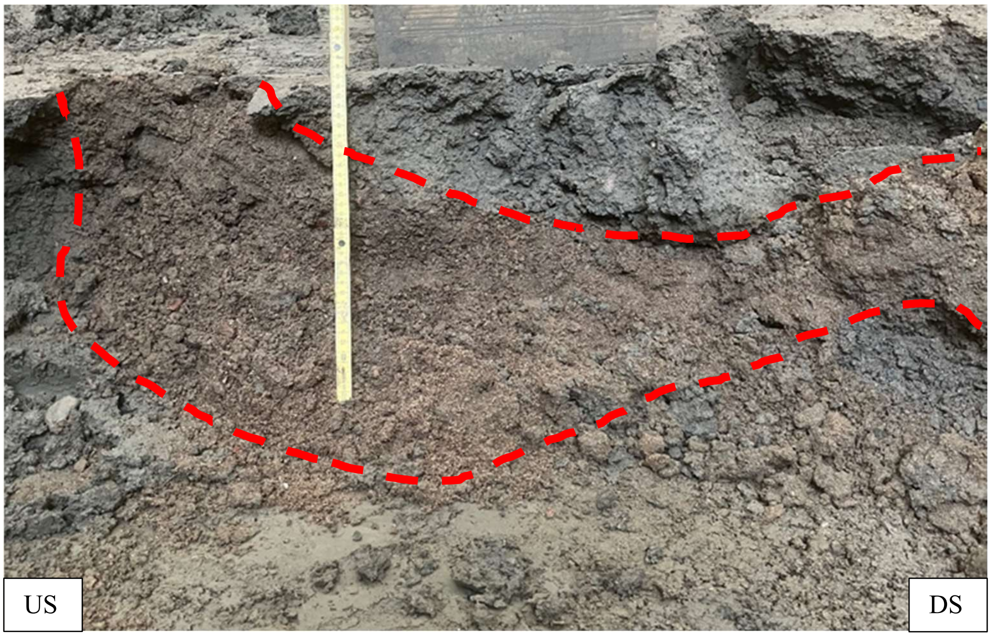

Figure 10. Eroded core soil found close to the wooden cube (between red, dashed lines). The material was coarser on the downstream side than on the upstream side, (Lagerlund and Riaz, 2026).

Along the right abutment, *a zone of disturbed material* was observed at a level of 0.5 m in the core, adjacent to the concrete wall. This zone extended across approximately one-third of the core's width, starting from the downstream fine filter, see Figure 11. Core soil from this area had lower content of fines, while the adjacent downstream fine filter had an elevated content of fines.

Figure 11. To the left: Sinkhole-like features found at the abutment marked with red arrows, eroded core soil material removed. To the right: A part of the abutment has been removed by the excavator and eroded core soil removed so the damage could be seen, (Lagerlund and Riaz, 2026).

4.3 Filter enrichment and washout

Sieve analyses on the downstream fine filter showed big differences in fine content compared to when it was built, see Table 2.

Table 2. Content of fines in downstream fine filter at different depths, at both abutments and centrally in the dam. Content of fines from construction 2019 compared with content of fines from dismantling 2024, 4.5 years apart, (Lagerlund and Riaz, 2026).

	% of fines				change over 4.5 years [%]		
Depth [m]	Left	Centre	Right	As built	Left	Centre	Right
1.2	6.2	7.9	6.4	6.1	2	30	5
1.6	6.4	7.6	6.7	4.4	5	25	10
1.9	4.4	8.4	13.4	6.9	-28	38	120
2.3	7.4	7.4	7.3	7.4	21	21	20
2.6	6.9	8.6	5.7	5.7	13	41	-7
3.0	4.5	8.8	9.5	5.5	-26	44	56
3.4	6.6	7.4	7.9	6.5	8	21	30
3.8	8.1	8.3	9.6	7.2	33	36	57

In the central section, fines content increased by up to 120% compared to the as-built condition. Downstream both the left-abutment and central horizontal defect, extra sieve analyses were made. Here, the downstream fine filter had about 50% less fines at the abutment, but 330% more fines near the central horizontal defect (results not included in Table 2). The downstream fine filter adjacent to the vertical defect and sandy zones showed moderate enrichment, while some areas near the right abutment had fewer fines. At the bottom of the downstream coarse filter, a lot of fines from the core were found (brown fines from the core were easy to tell apart from the grey fines from the filters and rockfill).

4.4 Erosion streaks between core soil layers

Thin streaks filled with sand were seen between core soil layers, especially near the downstream side, see Figure 12. These early signs of erosion were found in several places in the lower third of the core. In one case, when a block of core soil was turned over, a thin layer of sand was found underneath, showing erosion along the layer boundary.

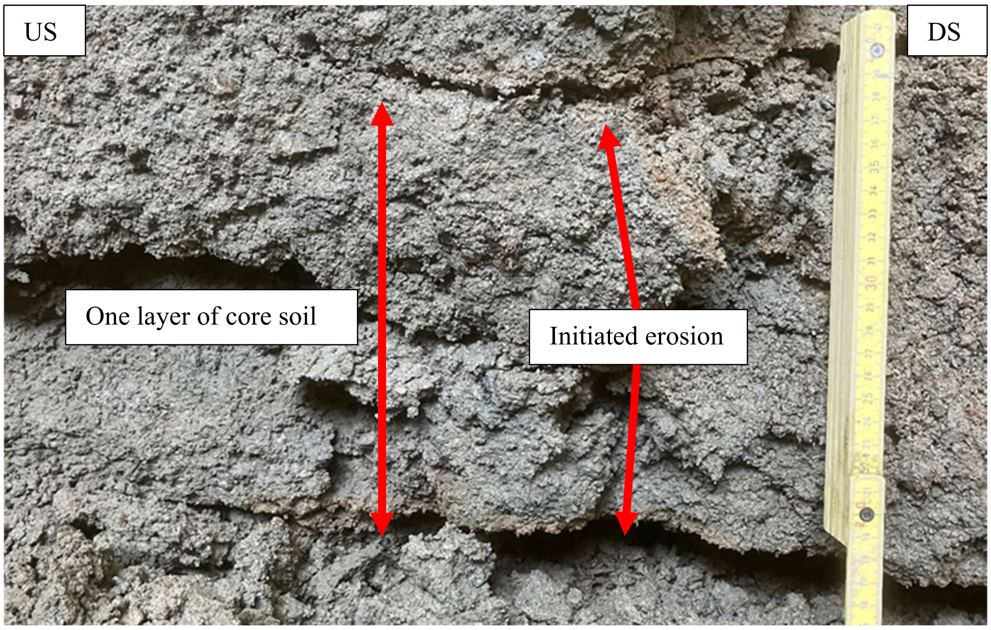

Figure 12. Internal erosion, at a very early stage, found in the layer boundaries between the core soil layers close to the downstream fine filter, (Lagerlund and Riaz, 2026)

4.5 Density measurements and core inhomogeneities

Dry density and water content tests performed at time of dismantling showed that *compaction quality varied in different parts of the core*, see Figure 13 and Figure 14.

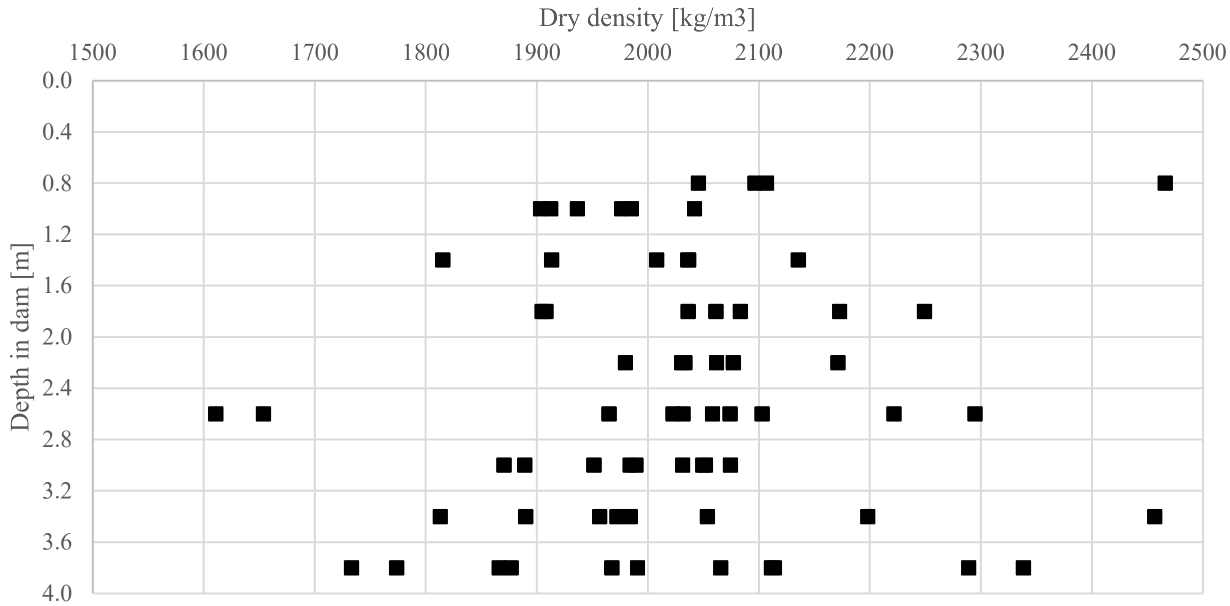

Figure 13. Dry density of core soil from different depths measured during the in-situ density tests at time of dismantling. Note the extreme points > 2.2 t/m³.

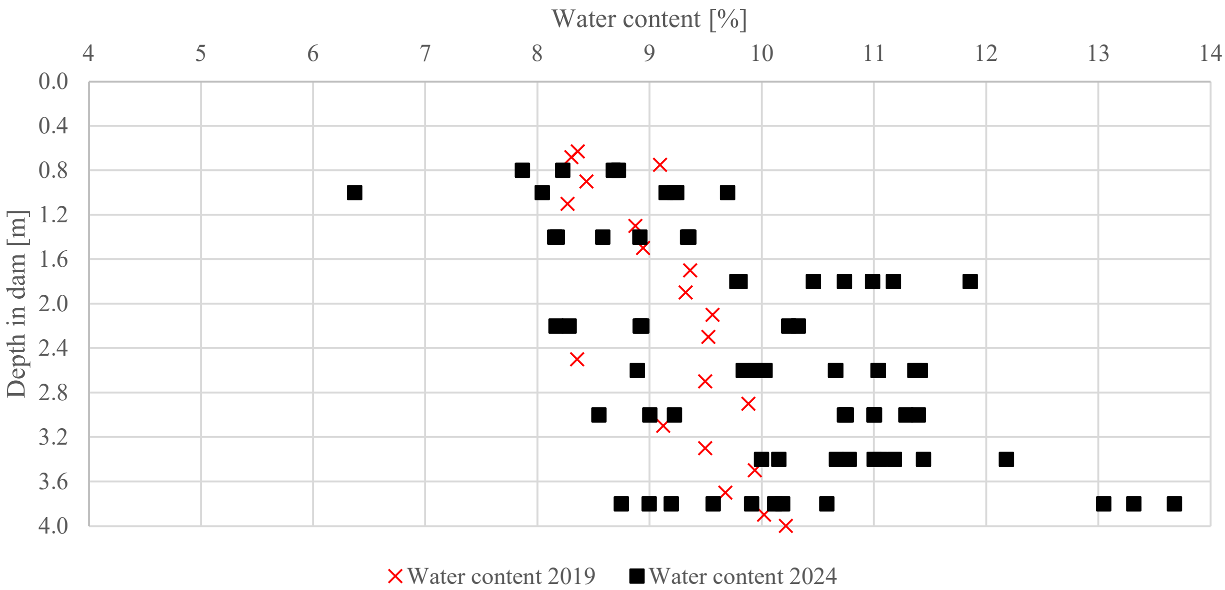

Figure 14. Water content of core soil from different depths measured during the in-situ density tests at time of dismantling. Water content at time of construction in 2019 was ~8 – 10.2%.

Key findings were:

- In some wet areas, the compaction was measured to be over 100% (optimum from testing prior to construction was 2200 kg/m³). The issue was found to be caused by soft core soil at the measurement site; when the water volumetric device was used, the soil caved in under its load. As a result, the volume of the hole was underestimated, which in turn produced an artificially high density value. However, the water content measurements remained unaffected by this error.

- Visual checks showed that the core had uneven parts, with wet and dry layers and clear lines between them and distinct stratification at layer boundaries.

5 Discussion

The internal erosion features observed in the Älvkarleby test embankment dam are attributable to a combination of design vulnerabilities, construction-induced heterogeneities, and material mismatches.

5.1 Settlements and vertical deformation

The core crest settled by up to 10 cm, and all recovered piezometers had moved down, showing vertical changes inside the dam (Table 1). Settlement of the core crest and found internal erosion features are shown in Figure 15.

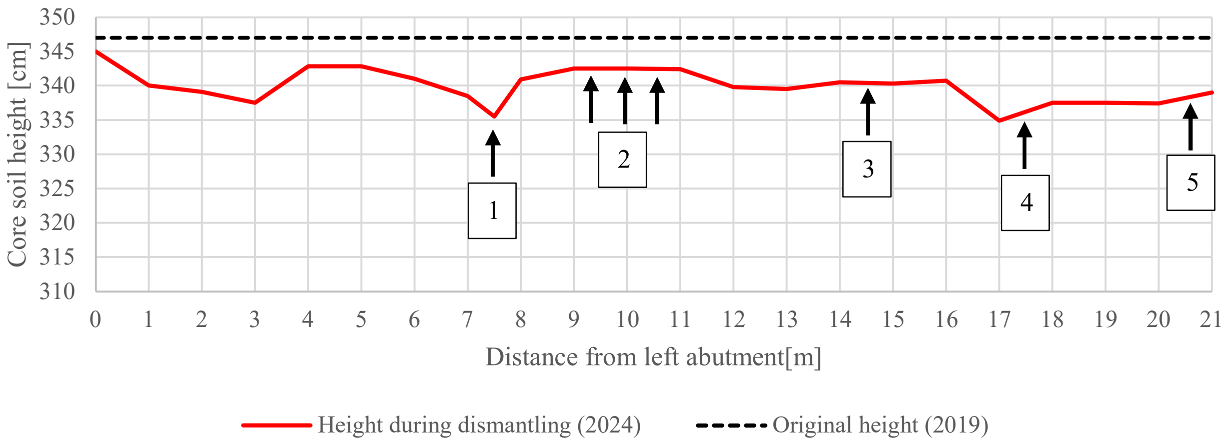

Figure 15. Settlements of the core crest with found erosion features highlighted, i.e., (1) three horizontal erosion pipes under vertical installed defect, (2) thin streaks filled with sand were seen between core soil layers, (3) sandy zone, (4) developing sinkhole-like feature, and (5) zone of disturbed material at right abutment.

The most pronounced displacements occurred where the three horizontal erosion pipes underneath the installed vertical defects (Figure 9) were found and where the sinkhole-like feature and horizontally installed strain cables were located (Figure 7 right). These strain cables, even though sealed with bentonite, likely made compaction harder and created weak spots where water could flow more easily. Similar effects of embedded elements on internal erosion susceptibility have been noted in previous studies, e.g., Fell and Fry (2007), Foster *et al.* (2000). Pore pressure monitoring during both initial impoundment and during the five controlled reservoir drawdown-refill cycles revealed anomalous behaviour in this zone. During the first impoundment it took ~1 year for the pore pressures to build up (Toromanović *et al.*, 2022b). During the drawdown-refill, the bottommost downstream piezometer in the core soil on the downstream side of the core exhibited a significant and persistent drop in pore pressure following the second fluctuation. The values did not return to the levels they had before (Toromanović *et al.*, 2025). This was interpreted as evidence of a developing preferential seepage path or internal erosion channel, allowing water to bypass the sensor location and preventing normal pressure build-up (Toromanović *et al.*, 2025). In contrast, the bottommost upstream piezometer in the core soil showed slightly elevated residual pore pressures after the third and subsequent cycles, suggesting locally impeded drainage or reduced hydraulic conductivity. These different results show a complex response inside the dam, where softening and shifting of stress likely caused the changes.

The saturated and softened condition of the soil beneath the sinkhole, observed during dismantling, aligns with these findings. The problem in this area was not high pore pressure, but a local loss of strength caused by erosion and water flow reducing the stress. These observations reinforce the importance of careful design and sealing of embedded elements, as well as the value of high-resolution pore pressure monitoring in identifying early signs of internal erosion. However, in three other locations where the strain cable traversed the core soil, the bentonite sealing had functioned as intended.

The water content measurements in the core soil at the time of dismantling were generally consistent with or slightly higher than those recorded during construction. This indicates that the draining of the reservoir did not significantly increase drying of the core. Therefore, the observed settlements are unlikely to have been caused by shrinkage due to drying; instead, they are more plausibly attributed to internal erosion and associated stress redistribution within the dam body.

5.2 Erosion features and flow paths

The way particles were sorted in the sinkhole, with coarse material at the bottom and fine particles at the top, matches what happens when water flow slows down during erosion. As seepage mobilizes core soil material, fine particles remain suspended longer and are thus transported further, while coarser grains settle earlier. This resulted in stratified deposit, with a coarse lag at the bottom and finer sediments accumulating above (Robbins *et al.,* 2020; Fell and Fry, 2007). This pattern has been documented in both field and laboratory studies. For example, sand boils formed during backward erosion piping often display similar grain-size stratification, with coarse particles near the vent and finer material deposited further away or higher up in a vertical profile (Robbins *et al.*, 2020). Hagerty (1991) also described how seepage-induced sapping and piping selectively remove fines, leaving behind coarser particles that can partially clog or stabilize erosion paths. The observed grain-size curves in Figure 8 align with these mechanisms, showing a clear decrease in particle size with elevation in the sinkhole fill.

The vertical coarse column defect exhibited erosion at both its top (at the core crest) and base (at level 1 m), with three horizontal erosion pipes extending along core soil layer boundaries (Figure 9). These layer boundaries, which are weak because they don't bond well (Fell and Fry, 2007), likely helped water move sideways once it entered the vertical defect. The bidirectional erosion pattern implies that the defect acted as a conduit under varying hydraulic gradients (Toromanović *et al.*, 2025).

Contrasting responses were observed at the two horizontal high permeable defects. The left-abutment defect, terminating at the concrete wall, was associated with a ~50% reduction in content of fines in the adjacent downstream fine filter, indicating unfiltered seepage along the core–abutment interface. In contrast, the centrally embedded defect showed fines enrichment in the downstream fine filter, suggesting partial retention of migrating particles. These results show how the shape of defects and nearby boundaries affect how water flows through the dam (Sherard *et al.*, 1984; ICOLD, 2017).

Additional erosion features, including a sandy zone near the wooden cube defect (Figure 10)and thin erosion streaks along core layer boundaries (Figure 12), further demonstrate the role of localised discontinuities. Although the sandy zone was located in proximity to the wooden cube, there was no physical connection between the two, and the wooden cube cannot be considered a contributing factor in its formation. The orientation of the sandy zone, sloping toward the downstream fine filter, suggests a localised hydraulic gradient or material discontinuity as the more plausible cause. The erosion streaks, particularly in the lower core, align with horizontal construction layers and suggest early-stage internal erosion.

At the right abutment, multiple small sinkholes and fines depletion in the core, coupled with fines accumulation in the adjacent downstream fine filter (Figure 11), indicate internal erosion along the core–structure contact. Achieving a perfect seal between compacted core and a rigid concrete abutment is known to be challenging, even with bentonite mastic applied (Fell and Fry, 2007; Lowe, 1997). In contrast, at the left abutment no signs of internal erosion were observed, underscoring inherent local variability in an ostensibly homogeneous dam, i.e., despite identical construction at both abutments, subtle differences can result in one side eroding while the other remains stable. By the time of dismantling (after ~4.5 years), the right-abutment erosion had propagated roughly one-third into the downstream portion of the core—a snapshot of the process, not an indication that progression was complete. Therefore, rather than a universal "constrained flow" artifact of the test setup, we interpret the right-abutment erosion as a localized phenomenon triggered by a specific vulnerability at that interface. It offers a cautionary insight that even when abutment contacts are built to standard, minor imperfections can lead to localized internal erosion, although factors like scale and boundary conditions should be considered when extrapolating to full-scale dams.

5.3 Filter performance and fines migration

Sieve analyses showed that the amount of fines in the downstream fine filter varied a lot in different places. In the central section, content of fines increased by up to 120% relative to the as-built condition, showing that the filter held back some of the eroded core particles. However, this accumulation may have reduced filter permeability, altering local hydraulic conditions. Conversely, the ~50% fines loss behind the left-abutment defect suggests filter failure, allowing unimpeded transport of eroded material (Lagerlund and Riaz, 2026).

While Chrysikou (2025) identified levels 1.2 m and 2.4 m as critical due to filter–core incompatibility, the present analysis attributes the observed erosion more directly to construction-induced deviations. Specifically, the as-built fine filter was coarser than designed, and the core soil finer, reducing retention capacity, see Figure 16. Even filters nominally compliant with RIDAS (2012) criteria exhibited erosion, showing that just following the design is not enough without good quality checks during construction (RIDAS, 2020; Sherard *et al.*, 1984). Due to time constraints and lacking man power on site, proper reception control of received construction material, i.e., sieving, of delivered core soil and fine filter were done after the construction.

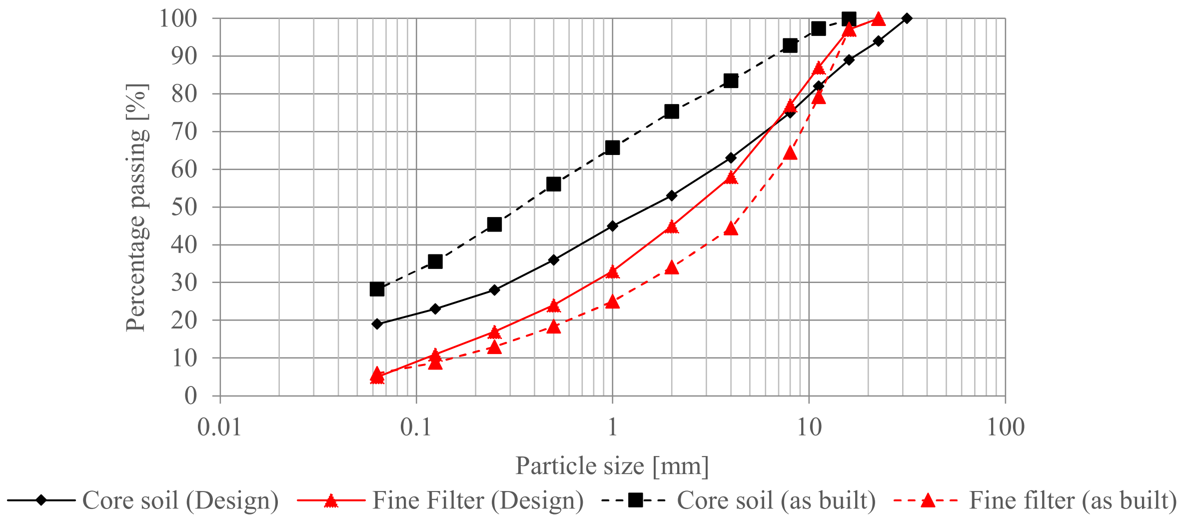

Figure 16. Core soil and fine filter particle size distribution at design and construction respectively.

Field observations confirmed that uniform placement of the coarse filter was unachievable. The broad gradation and dry placement conditions led to segregation, with coarser particles accumulating in pockets and finer fractions migrating downward due to gravity. Segregation of sand–gravel filters is well-documented (Rönnqvist *et al.*, 2020), and is known to create localised zones of high permeability. These zones can induce contact erosion at the fine–coarse filter interface, initiating a progressive erosion sequence.

5.4 Two-stage internal erosion mechanism

The way fines were lost in some places and built up in others can be explained by a two-step erosion process. In the initial stage, enrichment of the fine filter with fines from the core decreases the drainage capacity of the downstream fine filter by reducing its permeability. The clogged fine filter may have forced the water to take a different path, causing the phreatic line to intersect the coarse filter at a higher elevation. This increases the hydraulic load within the fine filter material. In the second stage, segregation or construction-induced discontinuities within the coarse filter create localized zones of insufficient retention capacity. These discontinuities facilitate the onset of contact erosion, allowing migration of fine particles from the adjacent fine filter into the coarse filter. This matches what Sherard and Dunnigan (1989) found, that filters with poor grain sizes or weak compaction are more likely to fail.

This hypothesis is supported, firstly, by field observations at both abutments, where a distinct imprint of the phreatic line was visible after 4.5 years of operation, see Figure 17. The imprint indicated that seepage was no longer being effectively drained through the fine filter but was instead emerging within the coarse filter. This observation suggests that the fine filter's drainage function had been compromised and that erosion of the fine filter into the coarse filter had likely occurred. Such a sequential failure mode, initial filter degradation followed by core erosion, has been conceptually described in ICOLD (2017), but to the authors' knowledge, this study is one of the first real examples of this process in an embankment dam. Secondly, the large amounts of eroded core soil material discovered at the bottom of the downstream coarse filter support the hypothesis that the downstream fine filter, at an unknown number of locations, has been compromised.

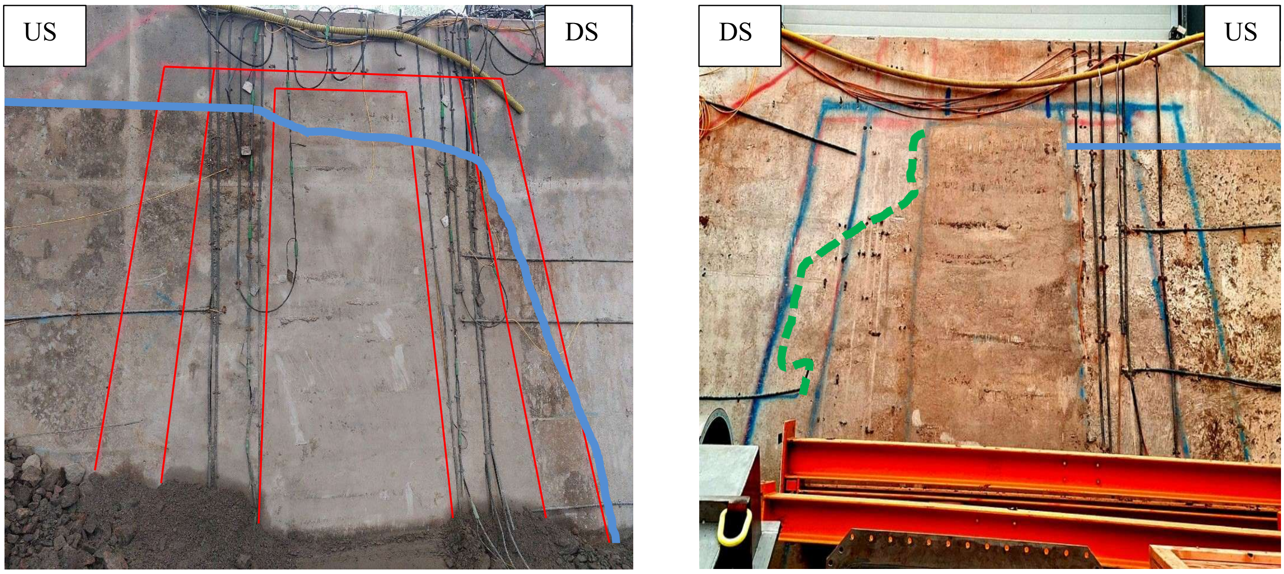

Figure 17. To the left: Left abutment with the inner zoning of the dam marked with red lines an phreatic line marked with a blue line. To the right: the right abutment. Inner zoning still visible from time of construction and phreatic line marked with blue line and the assumed phreatic line, downstream the core, marked with green dashed line (Lagerlund and Riaz, 2026).

At the abutments, however, the sharp soil–concrete interface represents a distinct boundary condition where preferential seepage may develop along the contact if the sealing is imperfect. The phreatic surface observed in Figure 17 therefore illustrates how contact flow at the abutments can locally bypass the fine filter and promote contact erosion at the soil–structure interface. However, this abutment-specific behaviour is not taken as direct evidence that the same mechanism governs seepage within the interior of the dam. Under normal conditions, seepage at the abutments would be expected to be effectively drained by the downstream fine filter. The abutment observations are therefore interpreted as a boundary manifestation of the process, complementing, rather than defining, the overall two-stage internal erosion mechanism inferred for the dam system as a whole.

This sequence is somewhat consistent with progressive erosion models involving contact erosion followed by concentrated leak erosion (Fell and Fry, 2007; ICOLD, 2017). At the left abutment, the coarse filter's separation from the fine filter at the concrete wall likely initiated fine filter erosion, followed by core erosion. In contrast, where filters remained intact, such as downstream of the central, high-permeability defect, erosion was limited, and fines were retained within the filter. This mechanism aligns with observations from other dam failures and experimental studies (Sherard *et al*., 1984; Rönnqvist *et al*., 2020) and provides a plausible explanation for the unexpectedly large volume of eroded material in the test dam.

5.5 Core compaction and inhomogeneities

Dry density and water content measurements revealed significant spatial variability in compaction quality, even in the same layer. Several zones, particularly in the lower part of the core, exhibited lower-than-expected dry densities. In saturated areas, degrees of compaction exceeded 100%, likely due to underestimation of sample volume during field testing, see Figure 18. These unusual results show that normal field tests don't always work well in soft, wet soils.

Figure 18. Imprint of field density measurement equipment on core soil from the same layer. To the left, the picture show very stiff core soil and very wet and soft to the right (Lagerlund and Riaz, 2026).

Lagerlund and Riaz (2026) proposed a model to explain the pronounced variability in core soil characteristics observed during dismantling. The idea is that the layering happened because of changes in compaction and moisture during construction. During construction in 2019, the core soil was wetter than its optimum water content, which limited the achievable compaction. Construction records indicate that the core was often placed with field values of water contents reaching 8 – 10.2%, compared to its optimum of ~6%. Prolonged compaction caused softening, requiring a reduction in compaction energy. As a result, the lower parts of each individual layer were often less compacted than the upper part, producing alternating layers of varying density and erodibility. These weaker layers, especially at layer boundaries, had more empty space and were easier to erode. Seepage preferentially followed these paths, promoting the formation of planar erosion features that could evolve into continuous flow channels as seen in Figure 12. The observed stratification and erosion patterns are consistent with findings from Foster *et al.* (2000), who linked poor compaction and moisture variability to internal erosion initiation.

The dismantling method further influenced the appearance of these layers. Excavation was performed in 0.4 m steps. In some areas, the excavator cut through the top of a layer where the soil was dense. In others, it entered lower in the same layer where the soil was softer. This led to apparent variability within individual layers. The observed heterogeneity supports the hypothesis that internal erosion can initiate in the absence of discrete defects, driven by stratified erodibility resulting from construction variability and uneven compaction. While dismantling may accentuate pre-existing heterogeneities, the alignment of erosion features with known construction challenges indicates that these weaknesses were intrinsic. These results show that it’s important to control moisture, prepare each layer well, and check the dam after building to reduce erosion risks.

5.6 Implications for current dam construction practice

The internal erosion features observed in the test dam developed despite careful construction and compliance with contemporary design practice. This highlights that internal erosion can be initiated by construction-induced heterogeneities, such as variable compaction, moisture-dependent density contrasts, material segregation, and imperfect filter–core transitions, even when current guidelines for embankment dam construction are followed. The findings therefore reinforce long-standing guidance that internal erosion is governed not only by design criteria, but critically by execution quality and verification during construction (Sherard et al., 1984; Fell and Fry, 2007; ICOLD, 2017).

The results do not imply that existing guidelines are inadequate, but rather demonstrate the difficulty of fully achieving their intent in practice. In particular, the observed filter performance and core erosion underline the importance of strict quality assurance of as-built conditions, including verification of compaction uniformity, moisture control, and filter gradation during placement. The fact that erosion initiated under relatively modest hydraulic gradients further suggests that dam susceptibility to internal erosion may be higher than often assumed if small construction deviations remain undetected. From a practical perspective, the findings emphasize that robust design standards must be complemented by rigorous construction control, documentation, and post-construction verification to ensure long-term internal stability.

6 Conclusions and recommendations

The dismantling of the Älvkarleby test dam showed that internal erosion happened in many places, even though the maximum global hydraulic gradient was only about 2. Erosion features included settlements, sinkholes, horizontal pipes, fines migration, and filter enrichment. These problems were caused by uneven construction, mismatched filters and core materials, and built-in defects.

Key findings include:

- Internal erosion started not just at known defects but also along horizontal joints between core layers, where stratification and insufficient compaction due to excessive moisture created zones of low density.
- Poor verification of incoming materials led to the wrong filter sizes being used for the core and fine filter.
- The downstream fine filter exhibited both fines enrichment and depletion, indicating variable retention performance. In some zones, coarse filter segregation enabled erosion of the fine filter. This subsequently exposed the core to unfiltered seepage and led to core erosion. These findings support the idea of a two-step erosion process.
- Excavation in 0.4 m steps revealed contrasting conditions within individual core soil layers. In some areas, the excavator cut through dense, well-compacted core soil material, while in others it exposed softer, more erodible zones. This difference shows both uneven construction and how the way the dam was taken apart affected what was seen.

These results demonstrate that even embankment dams constructed in accordance with modern guidelines may develop internal erosion due to construction-induced heterogeneities, underscoring the importance of rigorous construction control and verification of as-built conditions. Stratified erodibility, combined with localised hydraulic conditions, created preferential flow paths that led to erosion. This shows that just following the design is not enough and that better construction checks and follow-up inspections are needed.

Further work should focus on:

- Develop better ways to make sure compaction is even, even when moisture levels change, for example, using flexible compaction methods and real-time moisture checks.
- Study how uneven filter material placement can lead to erosion, using lab and field tests.
- Test the two-step erosion process in controlled experiments to confirm how it works.
- Study how erosion features change over time when water levels go up and down, to help improve dam safety checks.
- Look at how to combine construction records, dismantling data, and monitoring results to better spot early signs of erosion and understand what caused it.

These efforts will support the refinement of filter design, construction practices, and monitoring approaches, contributing to more resilient embankment dams.

Acknowledgements

The laboratory staff at the Vattenfall R&D laboratories, without you this project would never have been a reality.

Funding

The financial support by Vattenfall AB and Energiforsk AB is greatly appreciated and acknowledged.

Author contributions (CRediT)

JL: Main writer, responsible for both construction and dismantling of the dam, analyzing the results, project leader. PV: Writer, reviewing, analyzing the results. JT: reviewing, analyzing the results.

Use of AI

During the preparation of this work, the author(s) used copilot in order to verify references and proof reading. After using this tool/service, the author(s) reviewed, edited, made the content their own and validated the outcome as needed, and take(s) full responsibility for the content of the publication.

Data access statement

The data acquired in the study will be made available on request.

Conflict of interest (COI)

There is no conflict of interest.

References

Bernstone, C., Lagerlund, J., Toromanović, J. and Juhlin, C. (2021) 'Deformationer och portryck i en experimentell fyllningsdamm (Deformation and pore pressure in an experimental embankment dam)', Energiforsk Report 2021:772. Stockholm. (In Swedish)

Cederström, M. (1995) Expansion of Hydropower – A Historical Overview. Energiforsk Report 1995:2V. [Reprinted (2021)].

Chrysikou, V. (2025) Assessment of the filter criteria in an experimental embankment dam. MSc Thesis. Luleå University of Technology.

Dahlin, T., Olsson, P.-I., Rossi, M., Höglund, N. and Günther, T. (2019) Synthetic modelling of resistivity tomography for the construction of a test embankment. Lund University, Sweden.

Fell, R. and Fry, J.-J. (2007) 'The state of the art of assessing the likelihood of internal erosion', in Internal Erosion of Dams and Their Foundations. Proceedings of the 2005 International Workshop, Aussois, France. London: Taylor & Francis, pp. 1–24.

FERC (Federal Energy Regulatory Commission) (2021) Engineering Guidelines for the Evaluation of Hydropower Projects – Chapter R10: Internal Erosion and Piping. Washington, DC: Federal Energy Regulatory Commission.

Foster, M., Fell, R. and Spannagle, M. (2000) 'The statistics of embankment dam failures and accidents', Canadian Geotechnical Journal, 37(5), pp. 1000–1024. https://doi.org/10.1139/t00-030

Fry, J.-J. (2018) 'Lessons on internal erosion in embankment dams from failures and physical models', Keynote paper, 25th Meeting of the ICOLD European Club, Ljubljana, Slovenia.

Hagerty, D.J. (1991). Piping/sapping erosion. I: Basic considerations. Journal of Hydraulic Engineering, 117(8), pp.991–1008. https://doi.org/10.1061/(ASCE)0733-9429(1991)117:8(991)

ICOLD (2017) Internal erosion of existing dams, levees and dikes, and their foundations. Bulletin 164. International Commission on Large Dams.

Johansson, S. (1997) Seepage Monitoring in Embankment Dams. Doctoral Thesis. TRITA-AMI PHD 1014. Royal Institute of Technology, Stockholm.

Johansson, S. and Nilsson, Å. (2005) Erfarenheter från testfältet i Røsvatn – Intern erosion i fyllningsdammar. Elforsk Report 05:42. (In Swedish)

Johansson, S. and Sjödahl, P. (2018) Testdamm Älvkarleby – Modellering av termisk respons. HydroResearch AB. Vattenfall Report. (In Swedish)

Lagerlund, J. (2024) Grout Development and Methodology for Remedial Grouting of Embankment Dams. Doctoral Thesis. Luleå University of Technology.

Lagerlund, J. and Riaz, S. (2026) Dismantling, Documentation and Testing of the Älvkarleby Test Embankment Dam. Energiforsk Report 2026:1150.

Lagerlund, J. and Viklander, P. (2025) 'Dismantling a 4 m high experimental rockfill dam after four years of operation', Proceedings of the 31st Meeting of the European Working Group on Internal Erosion, Brno, Czech Republic.

Lagerlund, J., Bernstone, C., Viklander, P. and Nordström, E. (2022) Embankment Test Dam of Älvkarleby – Description of Installed Defects and Their Position. Mendeley Data, V3. https://data.mendeley.com/datasets/k7zrrbxxnb/3

Lowe, J. (1997) 'Slush grouting and contact treatment in embankment dams', Proceedings of the 19th International Congress on Large Dams, Florence, Italy. ICOLD.

Norooz, R., Nivorlis, A., Olsson, P.-I., Günther, T., Bernstone, C. and Dahlin, T. (2024) 'Monitoring of Älvkarleby test embankment dam using 3D electrical resistivity tomography for detection of internal defects', Journal of Civil Structural Health Monitoring, 14, pp. 1275–1294. https://doi.org/10.1007/s13349-024-00785-x

RIDAS (2012) Guidelines for dam safety. Svensk Energi – Swedenergy AB. (In Swedish)

RIDAS (2020) Guidelines for dam safety – Tillämpningsvägledning Kapitel 9. Energiföretagen Sverige. (In Swedish)

Robbins, B.A., Stephens, I.J., van Beek, V.M., Koelewijn, A.R. & Bezuijen, A. (2020). Field measurements of sand boil hydraulics. Géotechnique, 70(2), pp.153–160. https://doi.org/10.1680/jgeot.18.P.151

Rönnqvist, H., Girard, R., Lundin, J. and Viklander, P. (2020) 'The segregation of a sand-gravel dam filter of crushed rock and the influence of water content', Material Science & Engineering International Journal, 4(6), pp. 152–156. https://doi.org/10.15406/mseij.2020.04.00143

Sherard, J.L., Dunnigan, L.P. and Talbot, J.R. (1984) 'Basic properties of sand and gravel filters', Journal of Geotechnical Engineering, 110(6), pp. 684–700. https://doi.org/10.1061/(ASCE)0733-9410(1984)110:6(684)

Sherard, J.L. & Dunnigan, L.P. (1989). 'Critical filters for impervious soils.' Journal of Geotechnical Engineering, 115(7), pp. 927–947. https://doi.org/10.1061/(ASCE)0733-9410(1989)115:7(927)

Toromanović, J., Mattsson, H., Knutsson, S., & Laue, J. (2020). 'Geotechnical instrumentation of an experimental embankment dam', in J. Laue & T. Bansal (Eds.), Proceedings of the 4th European Conference on Physical Modelling in Geotechnics (ECPMG 2020), Luleå, Sweden, 15–17 March 2020, pp. 171–176.

Toromanović, J., Laue, J., Mattsson, H., Knutsson, S., Viklander, P. and Bernstone, C. (2022a) 'Observations from Initial Impoundment of an Experimental Embankment Dam – Field Data and Modelling', Proceedings of the 27th Congress on Large Dams, Marseille, France.

Toromanović, J., Mattsson, H., Knutsson, S. and Laue, J. (2022b) 'Mechanical behaviour of an experimental embankment dam during initial impoundment', Proceedings of the 20th International Conference on Soil Mechanics and Geotechnical Engineering (ICSMGE 2022), Sydney, Australia, pp. 1217–1222.

Toromanović, J. (2024). 'Monitoring and Modelling of Embankment Dams'. Doctoral Thesis. Luleå University of Technology, Luleå, Sweden.

Toromanović, J., Viklander, P. and Laue, J. (2025) 'Observations from cycles of varying reservoir levels on an experimental embankment dam', Proceedings of the 29th EYGEC, Rijeka, pp. 141–144.

Viklander, P., Lagerlund, J., Riaz, S. and Nordström, E. (2023) 'Non-destructive test methods for detecting defects in an experimental embankment dam', Hydropower & Dams, 30(3), pp. 74–79.